ISSN 1063-7745, Crystallography Reports, 2007, Vol. 52, No. 6, pp. 1030–1035. © Pleiades Publishing, Inc., 2007.
Original Russian Text © A.P. Menushenkov, O.V. Kashurnikova, R.V. Chernikov, G.Kh. Panova, A.A. Shikov, 2007, published in Kristallografiya, 2007, Vol. 52, No. 6, pp. 1067–1072.

QUASICRYSTALS

Local Structure of Binary Alloys $Zr_{70}Pd_{30}$

A. P. Menushenkov[a], O. V. Kashurnikova[a], R. V. Chernikov[a], G. Kh. Panova[b], and A. A. Shikov[b]

[a]*Moscow Engineering Physics Institute, Kashirskoe sh. 31, Moscow, 115409 Russia*
e-mail: menushen@htsc.mephi.ru
[b]*Russian Research Centre Kurchatov Institute, pl. Kurchatova, Moscow, 123182 Russia*

Received April 17, 2006

Abstract—The rearrangements of the local environment of zirconium and palladium atoms in the binary alloy $Zr_{70}Pd_{30}$ upon the transformation from the crystalline to the quasicrystalline and amorphous states were studied by extended X-ray absorption fine structure (EXAFS) analysis. In the quasicrystalline phase, the icosahedral environment was found to be formed only around the zirconium ions because of shifts of both the palladium and zirconium atoms to the center of the cluster; in addition, the structure of the icosahedral clusters is distorted. The transformation from the crystalline to the quasicrystalline phase is accompanied by the atomic rearrangement in the immediate environment of palladium, thus resulting in the partial displacement of palladium by zirconium. In the amorphous phase, the icosahedral short-range order is not observed. A model for the description of the structure of the quasicrystalline phase of $Zr_{70}Pd_{30}$ is proposed.

PACS numbers: 61.10.Ht, 61.44.Br

DOI: 10.1134/S1063774507060168

The quasicrystalline state was discovered more than two decades ago [1]. The character of ordering in this state is intermediate between that in the crystalline and amorphous states. The properties of the quasicrystalline state are not described in terms of classical crystallography. Although translational symmetry is absent, the long-range order in the spatial arrangement of atoms is retained, and rotational symmetry elements of forbidden orders are present. In spite of the fact that all components of quasicrystals, as a rule, are good metals [2], the specific resistance of quasicrystalline phases is an order of magnitude higher than the resistance of alloys in both the crystalline and amorphous phases, and the electron state density at the Fermi level has features of a pseudogap due, apparently, to electron localization at stable icosahedral configurations of atoms (clusters) [3]. The symmetry of clusters, in particular, the pentagonal symmetry, substantially differs from the crystal symmetry, a circumstance that is indicative of the formation of a new short-range order [4].

Both multicomponent and binary alloys show the ability to form quasicrystalline phases. The formation of a quasicrystalline phase, which has been recently observed in the binary systems $Zr_{70}Pd_{30}$ and $Zr_{80}Pt_{20}$ [5], is of particular interest because these results refute the earlier assumption that quasicrystallization can occur only in multicomponent zirconium-based alloys [6]. The $Zr_{70}Pd_{30}$ alloy can exist in the crystalline, quasicrystalline, and amorphous states without changes in the stoichiometry, and, in addition, it exhibits superconducting properties in all three phases, thus allowing an estimation of electron–phonon interactions [7]. At the same time, an analysis of electron localization at small-size clusters requires information on the local environment of atoms both in icosahedral clusters and between these clusters. To examine the changes in the short-range order resulted from crystal–quasicrystal–amorphous state phase transitions, in the present study we performed an extended X-ray absorption fine structure (EXAFS) analysis having high sensitivity to both the local environment of atoms and the elemental composition.

The $Zr_{70}Pd_{30}$ alloy was prepared at the Russian Research Centre Kurchatov Institute according to a known procedure [7] starting with electrolytically pure zirconium (99.99%) and pure palladium (99.96%). Polycrystalline samples of $Zr_{70}Pd_{30}$ were grown in an induction oven under argon. To prepare amorphous samples, the starting elements were placed in a boron nitride tube, melted in an induction oven under slight argon pressure, and rapidly quenched from the liquid state on the outer surface of a rotating copper cylinder. The quenching rate was estimated at 10^6 K/s. The resulting amorphous samples had a ribbon shape with a length of 1.5–2 mm and a thickness of about 30 μm. Quasicrystalline samples were prepared by annealing the amorphous ribbons under a stream of gaseous helium in a quartz tube placed in a muffle oven. The mode of the preparation of the most perfect icosahedral sample was optimized by performing annealing at several temperatures followed by rapid quenching. The X-ray diffraction analysis showed that crystalline phase has sp. gr. $I4/mmm$ with the unit-cell parameters a =

3.306 Å and c = 10.894 Å. The quasicrystalline phase was prepared at annealing temperatures of 740 and 760 K. The X-ray diffraction analysis revealed the presence of an icosahedral phase (sp. gr. $m\bar{3}\bar{5}$) with the hypercubic lattice parameter a = 7.624 Å. At the annealing temperature of 760 K, the quality of the resulting quasicrystalline phase was higher; however, the crystalline phase was detected in samples as the annealing temperature and time were further increased. The crystal structure was completely restored upon annealing at 873 K.

The EXAFS measurements were carried out above the Zr- and Pd-K edges (17998 and 24350 eV, respectively) at beamline A1 at the Hamburg Synchrotron Radiation Laboratory (HASYLAB, DESY) at 10, 77, and 300 K. The use of a channel cut crystal monochromator provided the energy resolution of about 2 eV at the Zr-K edge and about 2.5 eV at the Pd-K edge. The EXAFS spectra of single-crystalline samples with a substantial thickness were measured according to the fluorescence method. The EXAFS spectra of amorphous ribbons and quasicrystalline powders were measured in the transmission mode. The EXAFS spectra were processed using the VIPER program package [8] according to a standard procedure for the extraction and Fourier analysis of the EXAFS function $\chi(k)$. The simulation of the spectra was carried out using the equation

$$\chi(k) = -S_0^2 \sum_j N_j \frac{|f_j(\pi, k)|}{kR_j^2} \sin(2kR_j + \varphi_j(k)) \times \exp(-2\sigma_j^2 k^2), \quad (1)$$

where the summation was performed over all coordination spheres of the adsorbing atom, N_j is the coordination number, R_j is the average radius of the jth coordination sphere, and σ_j^2 is the Debye–Waller factor (the rms deviation of interatomic distances). The scaling coefficient S_0^2 accounts for the many-electron effects. The back-scattering amplitudes $f_j(\pi, k)$ and phases $\varphi_j(k)$ were calculated using the FEFF-8.20 program [9] for the structure of the Zr_2Pd crystal analog. In calculations of the amplitudes and phases for icosahedral samples, the atomic positions in the environment of Zr were slightly corrected to the icosahedral symmetry.

Figures 1 and 2 show the experimental EXAFS functions $\chi(k)k^2$ for a single crystal of $Zr_{70}Pd_{30}$ measured at T = 10 K above the Zr- and Pd-K edges, respectively, and the results of direct and inverse Fourier transforms along with the model EXAFS functions. For measurements above the Zr-K edge, the direct Fourier transform was performed in the range k = 3.5–14.5 Å^{-1} with the Kaiser–Bessel window function. The inverse Fourier transform was taken in the range R = 2.15–3.75 Å

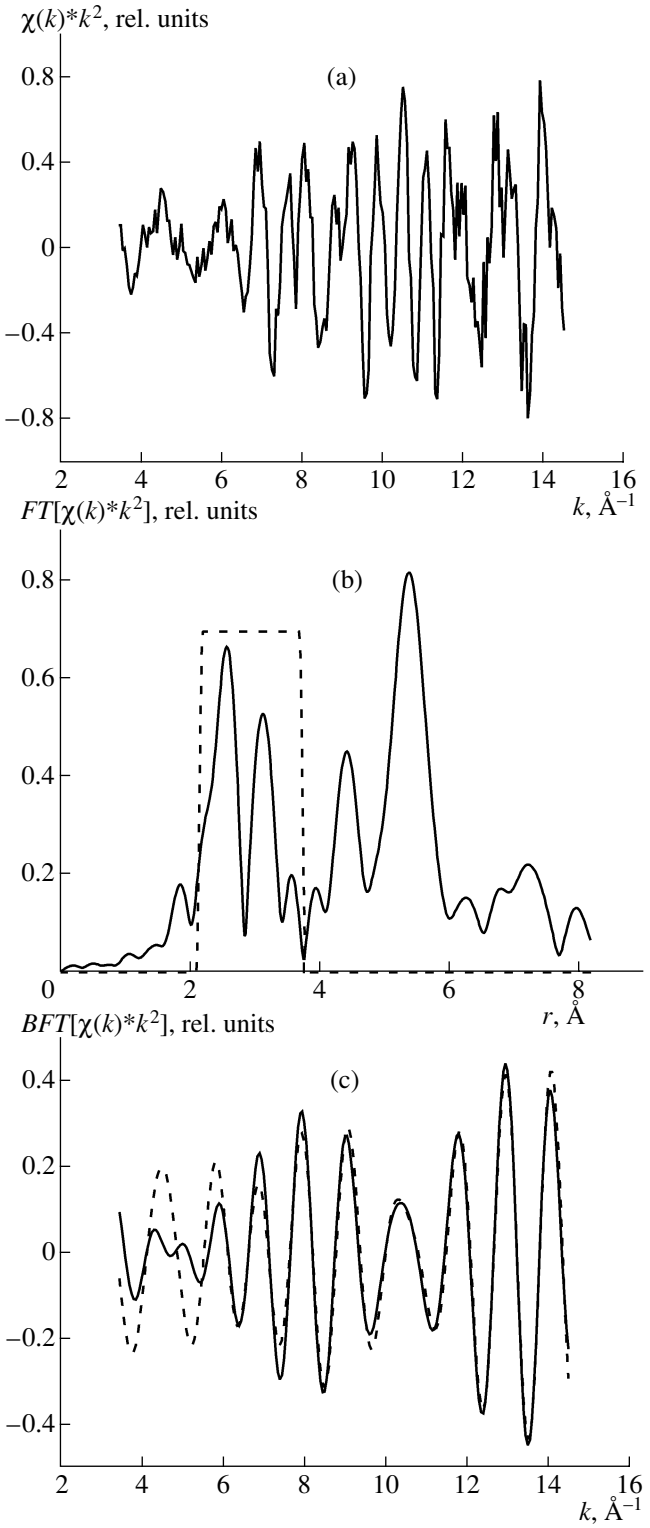

Fig. 1. (a) Experimental EXAFS function $\chi(k)k^2$ measured above the Zr-K edge for the $Zr_{70}Pd_{30}$ crystal at T = 10 K, (b) the Fourier-transform modulus of the EXAFS function $FT[\chi(k)k^2]$, where the window for the inverse Fourier transform for the extraction of the contribution of three nearest coordination spheres of zirconium is shown by a rectangle, and (c) the experimental (solid) and model (dashed) EXAFS functions for three nearest spheres of the local environment of zirconium.

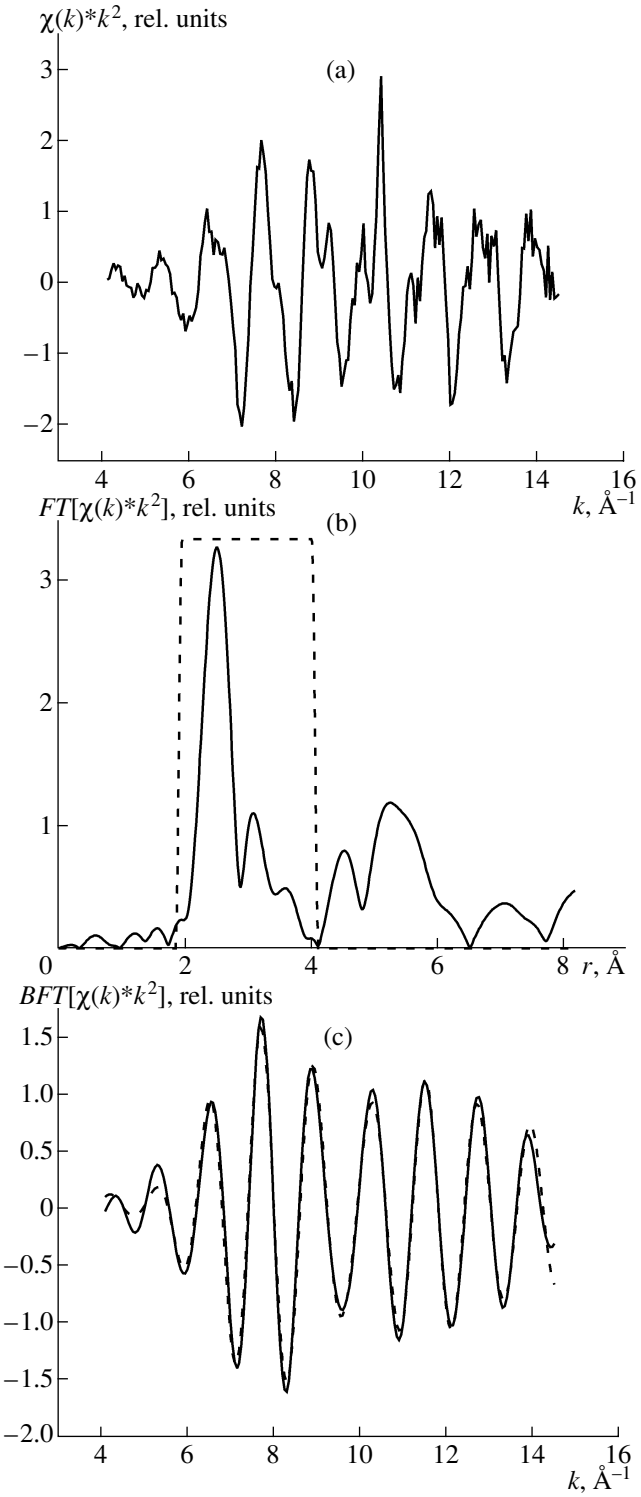

Fig. 2. (a) Experimental EXAFS function $\chi(k)k^2$ measured above the Pd-*K* edge for the $Zr_{70}Pd_{30}$ crystal at $T = 10$ K, (b) the Fourier-transform modulus of the EXAFS function $FT[\chi(k)k^2]$, where the window for the inverse Fourier transform for the extraction of the contribution of three nearest coordination spheres of palladium is shown by a rectangle, and (c) the experimental (solid) and model (dashed) EXAFS functions for three nearest spheres of the local environment of palladium.

with the use of the Hanning window function. For measurements above the Pd-*K* edge, the direct Fourier transform was performed in the range $k = 4.1$–14.5 Å^{-1}; the inverse Fourier transform, in the range $R = 1.9$–4.1 Å. The results of simulation of the EXAFS spectra are summarized in Table 1. The EXAFS analysis allowed us to refine the data on the crystal-prephase structure of $Zr_{70}Pd_{30}$ and to establish that this structure is similar to that of the Zr_2Pd crystal analog (Table 1).

Figure 3a shows the moduli of the Fourier images of the EXAFS functions measured above the Zr-*K* edge for the quasicrystalline and amorphous phases of $Zr_{70}Pd_{30}$ at $T = 10$ K. The modulus of the Fourier image of the EXAFS function for the quasicrystal substantially differs from that of the amorphous sample, a result that is indicative of the difference in the local environment of zirconium in the quasicrystalline phase and in the amorphous state. The further analysis showed that these differences are due to the appearance of icosahedral ordering around zirconium in the quasicrystalline phase. Then, we performed the inverse Fourier transform in the range $1.8 < R < 3.8$ Å. The results are presented as the experimental Fourier filtered EXAFS in Fig. 3b. This figure also shows the results of the simulation of the experimental EXAFS function for the quasicrystal that were obtained with two models. Model 1 includes the following three coordination spheres: one sphere consisting of Pd atoms at a distance of 2.70 Å and two spheres formed by Zr atoms at distances of 2.95 and 3.18 Å, respectively. Model 2 assumes the local ordering as the following two spheres: a sphere consisting of Pd atoms at a distance of 2.70 Å and a sphere formed by Zr atoms at a distance of 3.18 Å (Table 2). In the simulation, all three parameters (the coordination numbers, the interatomic distances, and the Debye–Waller factors) were varied. As can be seen from Fig. 3b, both models adequately describe the experimental EXAFS function. However, model 1 with the intermediate sphere of Zr atoms provides an estimation of the coordination numbers with smaller errors and gives a total coordination number of 11.5 corresponding to the icosahedral environment of zirconium. In this case, the structure of the icosahedral cluster is distorted. Thus, most of the Pd and Zr atoms are at distances of 2.70 and 3.18 Å, respectively, which is in good agreement with the electron-diffraction data [11]. The intermediate coordination sphere consisting of two Zr atoms is at a distance of 2.95 Å. The observed distortion can be attributed to the fact that not all zirconium atoms are centers of icosahedral clusters in the quasicrystalline structure and that the EXAFS data correspond to the average contribution of the local environment of Zr atoms occupying different crystallographic positions.

No icosahedral short-range order is observed in the environment of Zr in the amorphous phase (the results

of its simulation are presented in Fig. 3c and Table 2). The icosahedral short-range order in the amorphous $Zr_{70}Pd_{30}$ alloys was observed earlier by electron diffraction using the sharply focused electron beam in the nanometer region. EXAFS spectroscopy does not allow the observation of such regions.

Figure 4a shows the moduli of the Fourier images of the EXAFS functions measured above the Pd-*K* edge for the quasicrystalline and amorphous phases of $Zr_{70}Pd_{30}$. The Fourier transform was performed in the range $k = 3.9$–11.5 Å^{-1}. As can be seen from Fig. 4a, the modulus of the Fourier image of the EXAFS function for the quasicrystal differs only slightly from that of the amorphous structure, thus indicating the absence of local ordering about the palladium atoms in both phases. Figures 4b and 4c present the results of the inverse Fourier transform and the model EXAFS functions for the quasicrystalline and amorphous samples,

Table 1. Parameters for the nearest environment of the zirconium and palladium atoms in the crystal-prephase structure of $Zr_{70}Pd_{30}$ (the X-ray diffraction data for the structure of the Zr_2Pd crystal analog [10] are given for comparison; these data are marked with an asterisk)

Adsorption edge	Atomic type	N	R^*, Å	R, Å	σ^2, Å^2
K-Zr	Pd	4	2.887	2.86	0.0063
	Zr(1)	4	3.118	3.10	0.0044
	Zr(2)	4	3.309	3.29	0.0055
K-Pd	Zr(1)	8	2.887	2.86	0.0039
	Pd	4	3.309	3.29	0.0064
	Zr(2)	2	3.754	4.04	0.0045

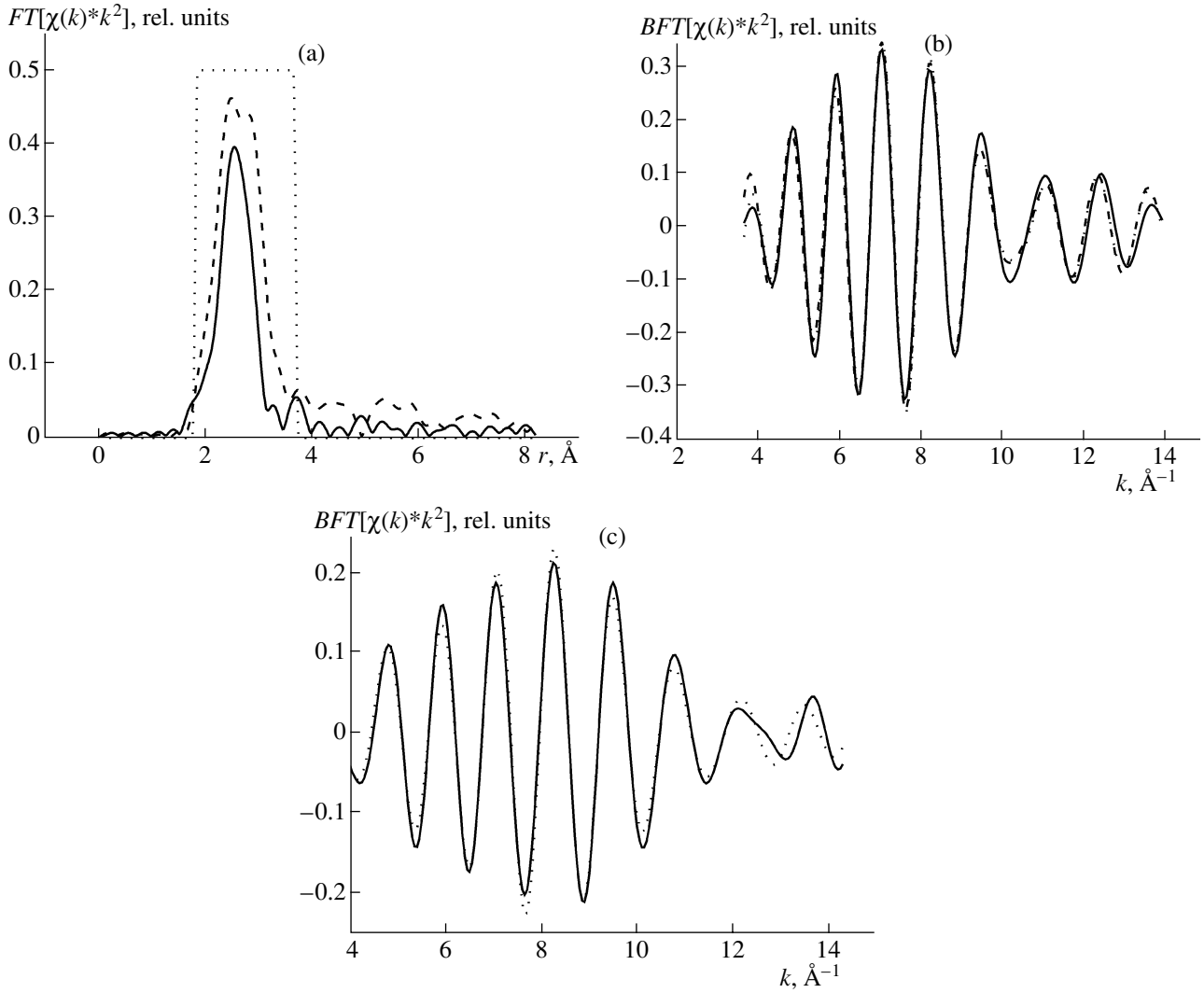

Fig. 3. (a) Fourier-transform modulus of the EXAFS function $FT[\chi(k)k^2]$ for the EXAFS spectra of the quasicrystalline (dashed line) and amorphous (solid line) samples of $Zr_{70}Pd_{30}$ measured above the Zr-*K* edge at $T = 10$ K, the window for the inverse Fourier transform for the extraction of the contribution of the nearest local environment of zirconium is shown by a rectangle, (b) the experimental (solid) and model (model 1, a dashed line; model 2, a dotted line) EXAFS functions for the icosahedral local environment of zirconium in the quasicrystalline state, and (c) the experimental (solid) and model (dashed) EXAFS functions for the nearest environment of zirconium in the amorphous state.

respectively, obtained in the range R = 1.70–2.25 Å. The results of the simulation (Table 2) provide evidence that the transformation from the amorphous to the quasicrystalline state is accompanied by the displacement of palladium atoms from the local environment of palladium.

A comparison of the parameters of the local environment of zirconium and palladium atoms led to the following conclusions about local atomic displacements during the transformation from the crystalline state to the quasicrystalline state (Tables 1 and 2):

(1) The main contribution to the formation of the icosahedral cluster about zirconium atoms is associated with displacements of palladium atoms (from 2.86 to 2.70 Å) and the nearest zirconium spheres (from 3.10 to 2.95 Å and from 3.29 to 3.18 Å) to the center of the cluster.

(2) The local environment of palladium completely loses the short-range order characteristic of the crystal structure, thus resulting in the transformation into the disordered (amorphous) state.

To summarize, the character of local atomic rearrangements in the $Zr_{70}Pd_{30}$ alloy that result from the crystal–quasicrystal–amorphous state phase transitions was determined by EXAFS spectroscopy. The intermediate sphere of Zr atoms in the icosahedral cluster having a distorted shape, the absence of icosahedral ordering about palladium atoms in the quasicrystalline state, and the displacement of Pd atoms from the local envi-

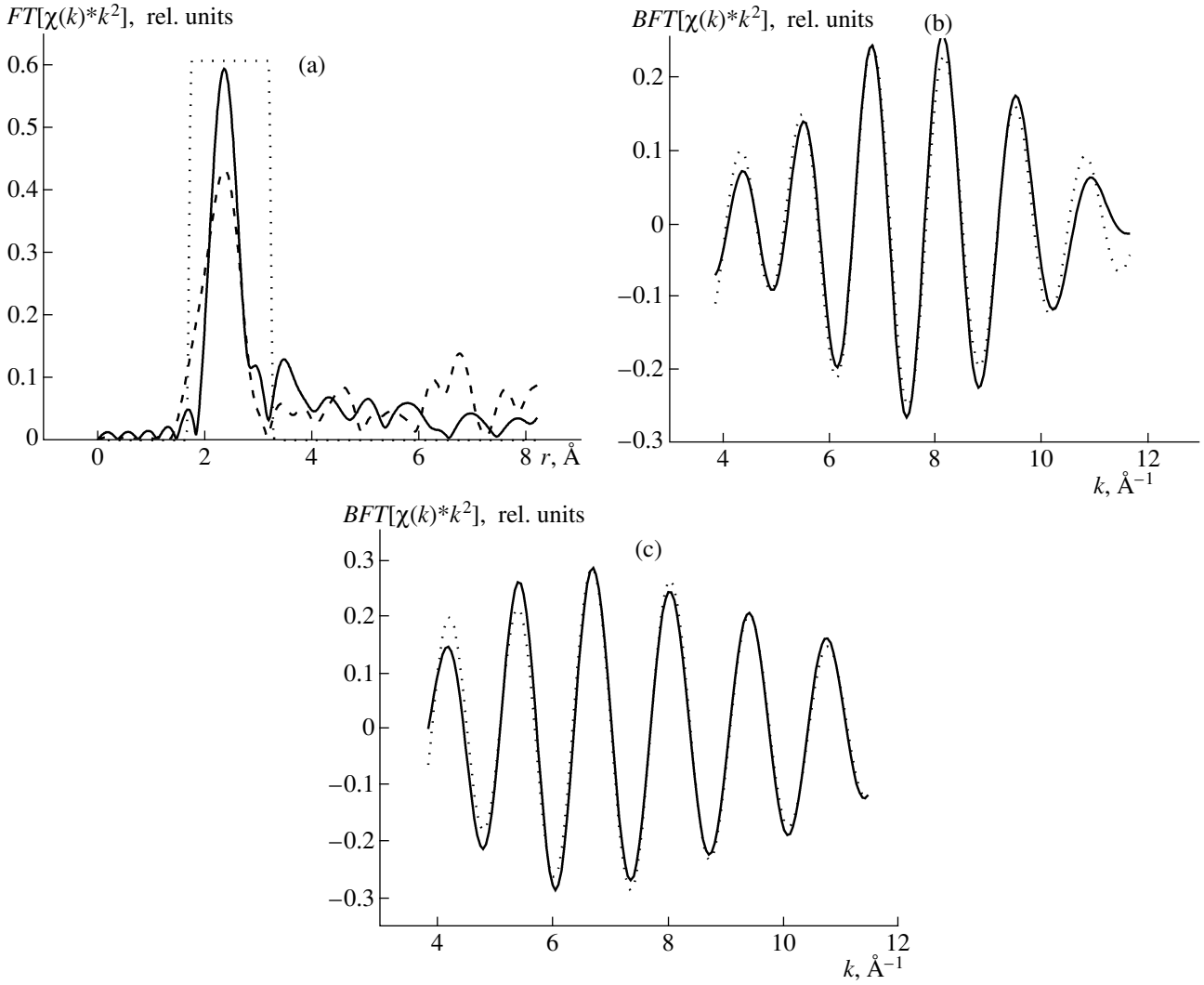

Fig. 4 (a) Fourier transform modulus of the EXAFS function $FT[\chi(k)k^2]$ for the EXAFS spectra of the quasicrystalline (dashed line) and amorphous (solid line) samples of $Zr_{70}Pd_{30}$ measured above the Pd-K edge at T = 10 K, the window for the inverse Fourier transform for the extraction of the contribution of the nearest local environment of palladium is shown by a rectangle, (b) the experimental (solid) and model (dashed) EXAFS functions for the local environment of palladium in the quasicrystalline state, and (c) the experimental (solid) and model (dashed) EXAFS functions for the nearest environment of palladium in the amorphous state.

Table 2. Parameters for the nearest environment of the zirconium and palladium atoms in the quasicrystalline and amorphous states of $Zr_{70}Pd_{30}$

Adsorption edge	Atomic type	N	R, Å	σ^2, Å^2
Quasicrystalline $Zr_{70}Pd_{30}$				
K-Zr, model 1	Pd	1.6 ± 1.0	2.70	0.0071
	Zr(1)	2.35 ± 1.0	2.95	0.0200
	Zr(2)	7.4 ± 1.0	3.18	0.0151
K-Zr, model 2	Pd	1.1 ± 1.0	2.70	0.0059
	Zr	6.4 ± 3.0	3.18	0.0147
K-Pd	Zr	3.9 ± 1.0	2.72	0.0122
Amorphous phase of $Zr_{70}Pd_{30}$				
K-Zr	Pd	1.3 ± 1.0	2.73	0.008
	Zr	2.3 ± 1.0	3.16	0.0124
K-Pd	Zr	2.9 ± 1.0	2.73	0.0077
	Pd	2.3 ± 1.0	2.83	0.0120

ronment of palladium upon the formation of the quasicrystalline order were found.

ACKNOWLEDGMENTS

We thank the HASYLAB User Committee for allowing us to perform experiments on a synchrotron source. We also acknowledge K.V. Klement'ev for help in performing the experiments, N.A. Chernoplekov for helpful discussion and valuable advice, G.F. Syrykh for preparing the amorphous sample, and G.V. Laskova for performing the X-ray diffraction analysis of the samples.

This study was supported by the Russian Foundation for Basic Research (project nos. 05-02-16996-a and 04-02-16017-a).

REFERENCES

1. D. Shechtman, I. Blech, D. Gratias, and J. W. Cahn, Phys. Rev. Lett. **53**, 1957 (1984).
2. V. F. Gantmakher, Usp. Fiz. Nauk **172**, 1283 (2002).
3. A. F. Prekul, N. Yu. Kuzmin, and N. I. Shchegolikhina, J. Alloys Compd. **342**, 405 (2002).
4. J.-M. Dubois, Mater. Sci. Eng. **294–296**, 4 (2000).
5. B. S. Murty, D. H. Ping, M. Ohnuma, and K. Hono, Acta Mater. **49**, 3453 (2001).
6. J. Saida, M. Matsushita, and A. Inoue, Intermetallics **10**, 1089 (2002).
7. G. Kh. Panova, N. A. Chernoplekov, and A. A. Shikov, Fiz. Tverd. Tela (St. Petersburg) **47**, 1165 (2005) [Phys. Solid State **47**, 1205 (2005)].
8. K. V. Klementev, J. Phys. D: Appl. Phys. **34**, 209 (2001).
9. M. Newville, B. Ravel, D. Haskel, et al., Physica B **208–209**, 495 (1995).
10. A. J. Maeland, E. Lukacevic, J. J. Rush, and A. Santoro, J. Less-Common Met. **129**, 77 (1987).
11. T. Takagi, T. Ohkubo, Y. Hirotsu, et al., Appl. Phys. Lett. **79**, 485 (2001).

Translated by T. Safonova